Available online at www.sciencedirect.com
ScienceDirect
Materials Research Bulletin 43 (2008) 3130–3139
Materials Research Bulletin
www.elsevier.com/locate/matresbu

Formation and dissolution of copper-based nanoparticles in SiO_2 sol–gel film using heat treatment and/or UV light exposure

J. Massera [a,*], J. Choi [b], L. Petit [a], M. Richardson [b], Y. Obeng [c], K. Richardson [a]

[a] School of Materials Science and Engineering, Clemson University, Clemson, SC 29634, USA
[b] College of Optics, Center for Research and Education in Optics and Lasers (CREOL), University of Central Florida, 4000 Central Florida Boulevard, Orlando, FL 32816, USA
[c] Nkanea Technologies, Inc., 6440 Aylworth Drive, Frisco, TX 75035, USA

Received 25 July 2007; received in revised form 25 September 2007; accepted 7 November 2007
Available online 17 November 2007

Abstract

We report in this paper, results on the formation and dissolution of Cu-based nanoparticles in sol–gel SiO_2 thin films using heat treatment and UV light exposure, respectively. Using UV–vis-NIR spectroscopy, we have shown that Cu_2O nanoparticles can be generated by controlling the aging of the sol prior to film deposition while the Cu^0 nanoparticles can be synthesized using a heat treatment in H_2 atmosphere at 550 °C for 6 h. It has been also demonstrated that irradiation with an UV pulsed (Q-switched Nd:YAG) or continuous black ray UV lamp can dissolve these Cu-based nanoparticles with controlled, spatial selectivity. The mechanism of the dissolution process was found to be mainly thermal. Finally, we report a new analytical technique for detecting/confirming the presence of low densities of Cu nanoparticles in the films, based on a relative heat flow measurement of such films using a micro-thermal analyzer (e.g., TA Instruments μTA model 2990).

Keywords: A. Thin films; A. Optical materials; B. Sol–gel chemistry; D. Color centers; D. Optical properties

1. Introduction

Miniaturization of integrated circuits for speed and low power consumption is driving the semiconductor industry outside the realms of normal optical lithography. In parallel, the quest for finer line widths is constrained by economics and practical manufacturing problems such as mask defects and contamination. In addition to miniaturization, the semiconductor industry is changing some key materials to improve devices performance [1]. Currently, the advanced metallization processes involve Cu damascene metallization, which are cumbersome and prone to contamination of fabrication lines. For example, the process of creating Cu lines includes an electroplating step; the quality of the Cu lines produced from the plating process varies dramatically, depending on the additives found in the plating solution [1]. Furthermore, the patterning of the blanket metal deposits into lines involves a number of difficult and chemically intensive processes, such as dry etching and chemical mechanical polishing (CMP). In summary, the metallization process is a complicated and expensive process, fraught with process inefficiencies and device reliability concerns [2].

* Corresponding author Tel.: +1 864 656 1259; fax: +1 864 656 1099.
E-mail address: massera@clemson.edu (J. Massera).

0025-5408/$ – see front matter © 2007 Elsevier Ltd. All rights reserved.
doi:10.1016/j.materresbull.2007.11.007

There is a need for new semiconductor manufacturing processes to compliment structural and material changes and the proposed effort aims to demonstrate a novel means to realize such processes.

Direct definition of metal lines is attractive for several reasons, including potential ease of fabrication. However, despite over 30 years of work in various laboratories, high quality directly written metal structures have remained elusive. One of the primary reasons for this failure has been the use of thermal decomposition of precursors as the technical basis for metal direct-writing [1,2]. Currently, the methods available to obtain metallic particles dispersed in dielectric matrices include traditional melting-quenching and annealing, chemical vapor deposition, sputtering, ion exchange, as well as high energy particle (e.g., ion implantation) irradiation-assisted methods. These methods are attractive due to their easy controllability of size and density distribution of the nanoparticles [3–8]. However, the latter methods do not allow for strict spatial selectivity of the process, owing to largely unfocused beams of energy. The synthesis of metallic particles such as Pd [9,10], Cu [11,12], Ag [13] and Au [14] in SiO_2 coating have been previously demonstrated by the sol–gel route. To the best of our knowledge, the thermal characteristics of metallized SiO_2-based matrices, such as relative heat flow measurements, have not been previously reported. Furthermore, the present work pertaining to the manipulations of such Cu nanoparticles-containing films, including but not limited to, the UV light-assisted dissolution of these metallic particles, is believed to be the first reported.

In this paper, we report results on the formation and the dissolution of different Cu-based nanoparticles such as Cu_2O and Cu in SiO_2 matrices using UV exposure and heat treatment in different atmospheres. The effect of the Cu doping on the optical properties of the SiO_2 matrix is first discussed. We also present the effect of UV irradiation using a nanosecond laser or a continuous (cw) lamp and a heat treatment on the formation and dissolution of the nanoparticles. The most commonly used characterization tools to study nanoparticles in these films and in bulks have been X-ray diffraction, TEM and AFM. In our case, the study of the Cu-based nanoparticles has been investigated using a relative new technique developed in our group, which measured the relative heat flow using a micro-thermal analyzer. The surface profile of the investigated films has been, also, measured with a microscope profilometer and is discussed as a function of formation/dissolution of nanoparticles.

2. Experimental procedures

2.1. Sample preparation

Copper-doped sol–gel films with the generalized composition of xCu–$(1-x)SiO_2$ (with $x = 0$, 0.005 and 0.05) were prepared by the hydrolysis and condensation of high purity (98%) tetraethylorthosilicate (TEOS, $C_8H_{20}O_4Si$ from Sigma–Aldrich), using ethanol as a solvent. The metallic precursor used in this work was 98% pure copper(II) nitrate hemipentahydrate [$Cu(NO_3)_2{\cdot}xH_2O$, with $x \approx 5$–6] from Sigma–Aldrich. After stirring for few minutes, the solution was mixed with a solution containing the Cu metallic precursor dissolved in 10 ml of ethanol. Small aliquots of concentrated HCl were added to the mixture, as catalyst. The molar ratio of matrix precursor/ethanol/water/HCl was kept at 1:30:1:0.03. Depending on the test objectives, the final solution was sealed in a container and stirred continuously at room temperature for 24 h in ambient light or in the dark environment to avoid an ambient light oxidation of the native copper species.

Films were performed by spin-coating on clean and dried microscope slides. Typically, 15 layers were deposited at 1000 rpm for 10 s and then annealed at 150 °C for 15 h. The thickness of the films was measured to be 600 ± 100 nm using the Zygo New View White Light Interferometer 6300 microscope (Zygo Corporation, Middlefield, CT, USA). The final film thickness was found to be independent of Cu content of the sol–gel.

2.2. UV light source

2.2.1. Continuous wave (cw) UV lamp

The cw 366 nm source used during this study was a black ray lamp with a power of $2\times$ 6 W (UVL-56, UVP), with a spectral bandwidth of ~330 to 370 nm full width half maximum (FWHM). The films were exposed using this lamp for 24 h and the corresponding dose of UV light is about 420 J/cm^2.

2.2.2. Nanosecond (ns) pulsed laser

The other system used to irradiate the films was a commercial Q-switched Nd:YAG laser (Quanta-ray GCR-190, Spectra Physics) with a maximum laser pulse energy ~300 mJ at 1064 nm. The pulse duration was ~10 ns, and the repetition rate 100 Hz. The fundamental frequency was tripled to obtain 355 nm using type I potassium dideuterium phosphate (KD*P) crystal. The laser beam, with 7 mW power, was focused onto the film using a lens with focal length of 75 mm and the film was then moved towards the lens ~3 cm from the focus. The beam diameter was calculated to be 1 mm and the intensity at the film was obtained about 0.8×10^6 W/cm^2 and corresponding dose of UV light was ~1500 J/cm^2 for 30 min exposure.

2.3. Transmission measurement

The transmission spectra of the deposited films were measured with a dual beam UV–vis-NIR Perkin Elmer Lambda 900 spectrophotometer at a scan rate of 2 nm/s over the 200–800 nm spectral region. The measurements were performed at room temperature, and not corrected for Fresnel losses.

2.4. Surface profile characterization

The Zygo New View 6300 white light interferometer (Zygo Corporation, Middlefield, CT, USA) was used for characterizing and quantifying surface roughness, step heights, and other topographical features using 5× and 20× objectives. The ''High Pass'' filter was used and the filter type was set to ''FFT Fixed'', 160 μm was used as the filter low wavelength, and no geometry was removed.

2.5. Localized thermal conductivity/relative heat flow measurements

Local heat flow values on films deposited were determined using a micro-thermal analyzer (μTA) model 2990 from TA Instruments. This device incorporated a Pt/Rh Wollaston wire probe, which functioned simultaneously as both a resistive heater and resistive temperature detector (RTD). The probe was placed on an AFM head, which allowed high precision scanning in three dimensions. A temperature-controlled stage at 27 °C and a probe temperature of 127 °C were utilized in order to prevent variations caused by changes in ambient thermal conditions.

Surface scans were performed on each of three randomly chosen 50 μm × 50 μm areas, immediately followed by an identical reference scan in air at a constant height of ~200 μm above the sample surface. The reference scans were used as the non-contact signals for data analysis. Local relative heat flow maps were obtained by processing the scan data with ImageJ v1.63 software. As shown below, the relative heat flow value after processing was unit less:

$$\text{relative heat flow map (unit less)} = \frac{\text{surface scan map (mW/K)} - \text{reference scan (mW/K)}}{\text{surface scan map (mW/K)}}$$

The mean relative heat flow was taken from the histogram of the heat flow deviation data. The accuracy of the mean relative heat flow was estimated at ±0.01.

3. Results and discussion

The goals of the work described in this paper were (i) to investigate the possibility to form and dissolve in a spatially selective manner, Cu-based nanoparticles in silica-based thin films prepared by spin-coating of a sol–gel solution, using UV light exposure and heat treatment and (ii) to estimate the mean relative heat flow of the films as a function of the presence of Cu-containing nanoparticles.

In this first section we discuss the characterization of our sol–gel SiO_2 thin films. Specifically, we focus on the effects of Cu precursor addition in the SiO_2 matrix on the optical and thermal properties of the SiO_2 films. Fig. 1 compares the optical transmission spectra of the investigated films; seen is a monotonic decrease in the transmission properties which can be observed with an increase of x, the content of Cu introduced in the SiO_2 matrix. As seen in Fig. 1, the interference envelopes characteristic of interference related to back and front surface reflections are not pronounced for the spectrum of the film with $x = 0.05$ or missing in the spectra of the films with $x = 0$ and 0.005 from

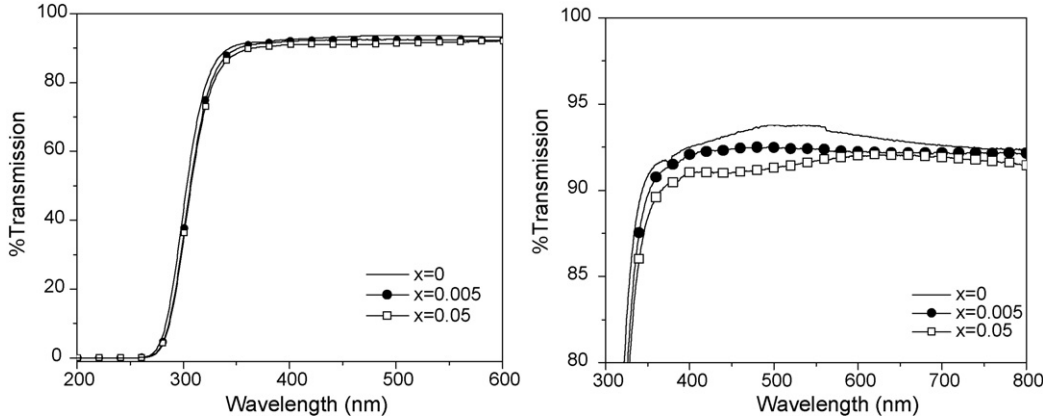

Fig. 1. Transmission spectra of Cu-doped SiO_2 films prepared with $x = 0$, 0.005 and 0.05 (a) and (b) is the zoom in to exhibit the small interferences.

the typical oscillations in transmission, probably due to the small thickness of the films and to the low index contrast between lightly doped films and the substrate. It is very well known that (i) the upper and lower interference envelopes are dependent on the refractive index and (ii) the distance between the fringes is dependent on both the refractive index and the thickness of the films [15].

The surface profile of the investigated films has been measured using the Zygo New View white light interferometer microscope and a micro-thermal analyzer. Not presented in this paper, we observed an increase of the film surface roughness to 30 ± 5 nm when x increases to 0.05. This increase of film roughness with the introduction of Cu has been already measured by Celik et al. who, also, observed an increase of the film roughness with increasing dopant concentration in Cu-doped TiO_2 dip-coated films [16]. Fig. 2a–c shows the relative heat flow (Q) maps of the three representative Cu-doped films (where $x = 0$, 0.005 and 0.05) investigated in this work. One can notice that the mean relative heat flow of the matrix areas on all three samples (0.17 ± 0.01) appear to be Cu concentration independent and uniform in a microscope slide scale and between films. Further examination of the scans of the film surface shows some surface defects, which can be responsible for the increase of the film roughness measured with the Zygo New View white light interferometer microscope. It is interesting to notice that these surface defects have a lower relative heat flow value $\sim 0.14 \pm 0.01$ than that of the surrounding film. This may indicate that these defects are Cu free. The relation between these Cu free SiO_2 aggregates and the concentration of Cu is still not completely understood and needs more investigation.

In order to decrease the film surface roughness, the films were annealed in air at 550 °C for 6 h. While no noticeable variation of the film optical properties was observed after the heat treatment, a dramatic decrease of the film roughness

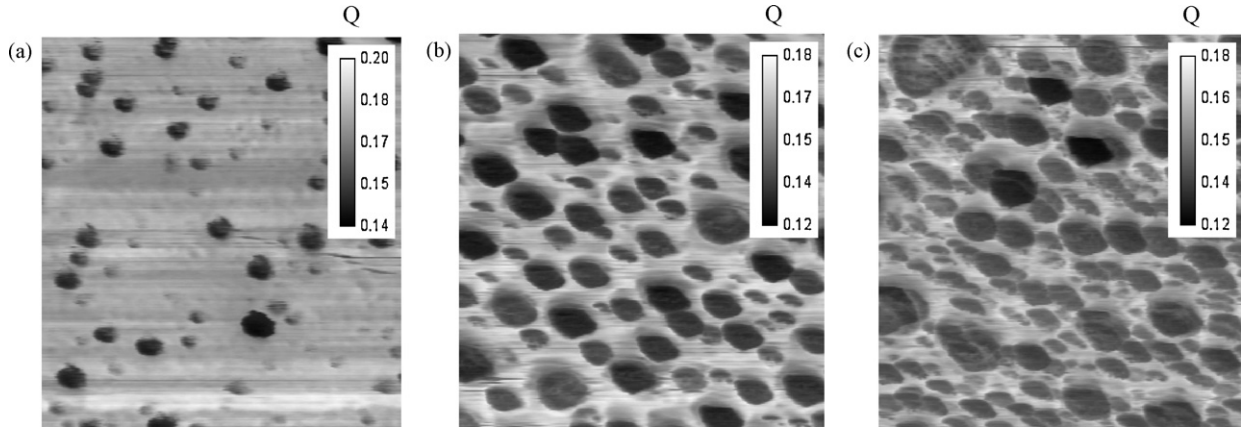

Fig. 2. Map of the relative heat flow of films with $x = 0$ (a), $x = 0.005$ (b) and $x = 0.05$ (c).

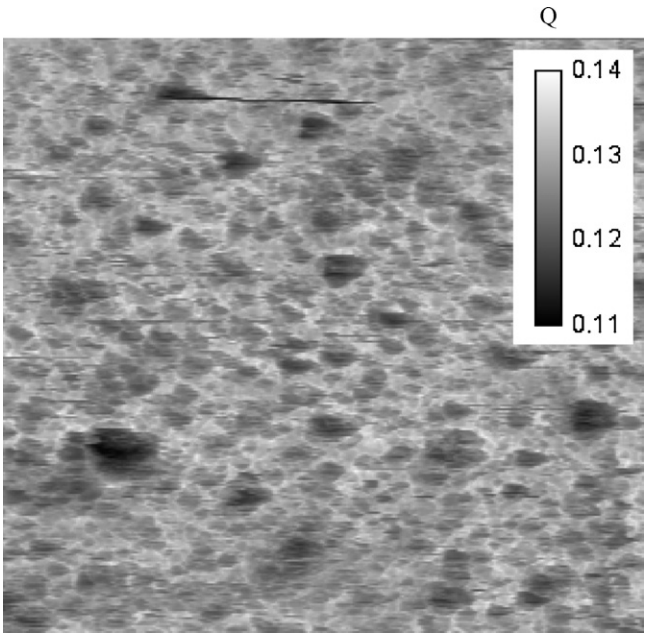

Fig. 3. Map of the relative heat flow of films with $x = 0.05$ after heat treatment in air at 550 °C for 6 h.

from 30 ± 5 to 13 ± 5 nm was measured for films with $x = 0.05$ and from 15 ± 5 to 7 ± 5 nm for the film with $x = 0.005$. This may be attributed to the solvent evaporation and/or the densification of the films.

Fig. 3 shows the map of the relative heat flow after the thermal annealing at 550 °C for 6 h of the film with $x = 0.05$. In accordance with a decrease of the film surface roughness, the heat treatment at 550 °C for 6 h decreases the number of the surface defects. It is also interesting to note that the mean relative heat flow of the film decreases uniformly from $\sim 0.17 \pm 0.01$ to $\sim 0.13 \pm 0.01$ after heat treatment. Cattaruzza et al. have shown that by heating Cu-doped silica films; it is possible to obtain samples, which contain only one kind of copper species such as copper monoxide nanoparticles or metallic nanoparticles [12]. Their thermal annealing was performed in air at 700 °C for 5 h to allow the formation of CuO particles at the surface of the film. Similar results have been obtained in Cu-doped TiO_2 [16]. For this reason, the decrease of the mean relative heat flow after heat treatment at 550 °C may be related to the densification of the films and/or to the probable formation of CuO nanoparticles at the surface of the film. This needs to be confirmed in our film and so, further investigations are ongoing.

3.1. Formation of copper nanoparticles

We now turn our attention to the formation of copper nanoparticles in the films. One of the purposes of the study is to verify if it is possible to form different Cu-based nanoparticles in SiO_2 thin films prepared by a sol–gel technique. Two techniques have been used.

In the first technique, the aging of the sol solution was varied from 30 min in ambient light to 1 day in dark environment before the film deposition. The transmission spectra of the films are shown in Fig. 4. One can notice that when the solution is aged for 30 min in ambient light, the transmission spectrum of the corresponding film shows an absorption band at 450 nm, which is not present in the spectrum of the film deposited from solutions aged for 24 h in the dark. This band may be attributable to the presence of Cu_2O nanopaticles in the film in agreement with [17]. The position of the maxima of this band is 450 nm with a shoulder at 475 nm, which is in good agreement with positions of the absorption bands of Cu_2O particles in silica matrix. The 475 nm shoulder can be attributed to the blue-shifted $n = 1$ exciton transition of the yellow series of Cu_2O particles while the band at 450 nm can be attributed to the blue-shifted $n = 1$ exciton transition of the green series [18]. It is conceivable that these nanoparticles were already in the sol–gel solution, and may have been formed due to light-induced oxidation of the dopant precursor in the solution.

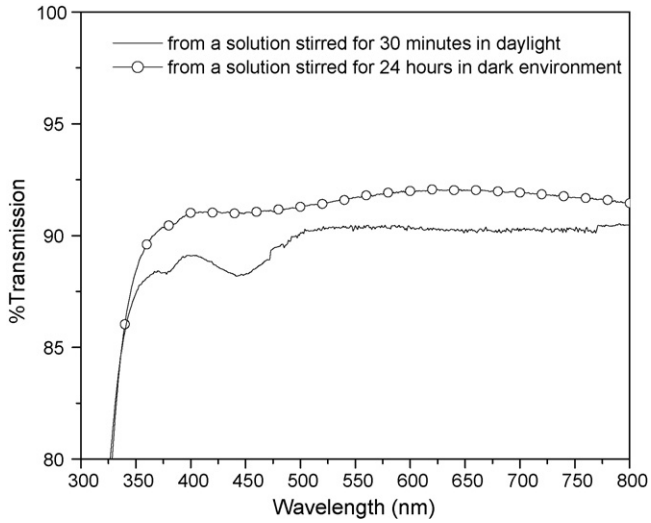

Fig. 4. Transmission spectra of films with $x = 0.05$ from a solution stirred for 30 min in daylight and for 24 h in dark environment.

Using the films from solutions aged in the dark, we produced Cu nanoparticles by heating up at 550 °C for 6 h in a reducing atmosphere such as an Ar stream with a mixture of H_2 at 5%. After heat treatment, the color of the film with $x = 0.05$ changed from colorless to brownish. The transmission spectra of the film before and after the heat treatment are presented in Fig. 5. The heat treatment in H_2 atmosphere decreases the transmission properties of the film. Moreover, one can notice that a new band at around 580 nm, also, appears. In agreement with previous studies where the formation of Cu nanoparticles using the same reducing atmosphere has been seen in Cu-doped silica films [11,19,20], this band can be attributed to the characteristic peak associated with a surface plasmon resonance for Cu nanoparticles. An annealing in hydrogen results in reduction of Cu(I,II) to Cu(0) that is aggregated in the form of Cu nanoparticles [18]. Due to the position at 575 nm of the absorption band related to the Cu nanoparticles, the Cu nanoparticles are expected to have a diameter at ∼51 nm in agreement with [18] who related the size of the Cu nanoparticles measured with a TEM to the position of the absorption band related to Cu nanoparticles. However, compared to these studies where the heat treatment was performed in the range 700–1000 °C for a period of time

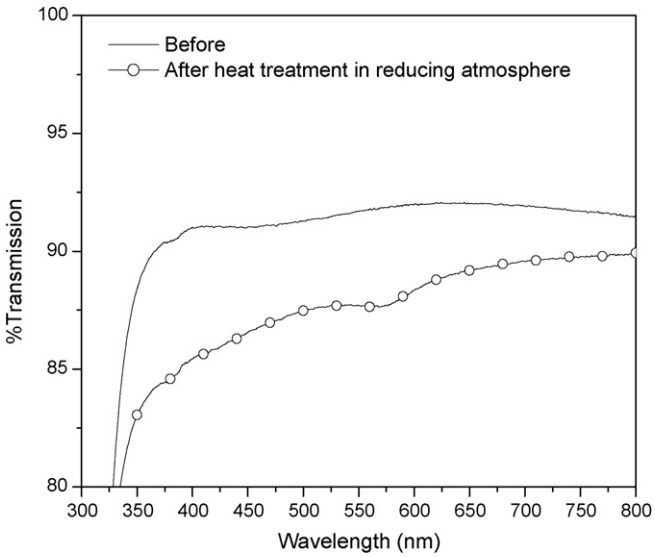

Fig. 5. Transmission spectra of films with $x = 0.05$ before and after heat treatment in reducing atmosphere for 6 h at 550 °C.

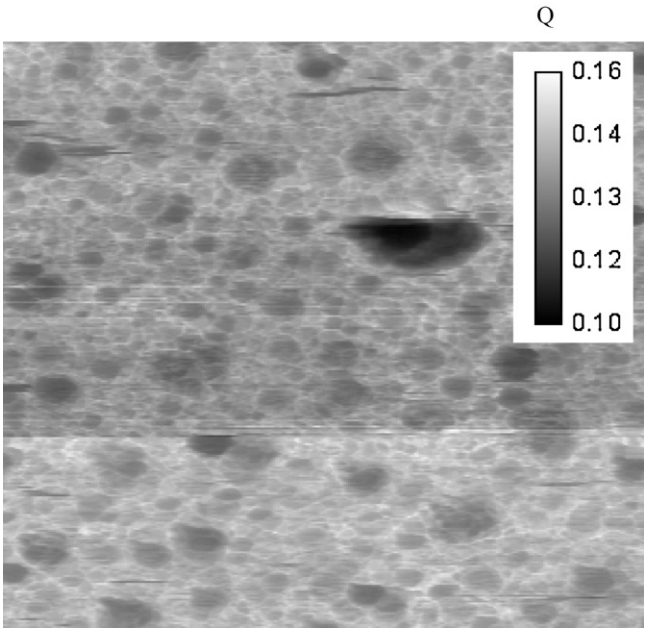

Fig. 6. Map of the relative heat flow of the film heat-treated in H_2.

between 1 and 2 h, we show that it is possible to form these Cu nanoparticles at a lower temperature if the heat treatment is extended to a longer period of time (6 h).

The surface profiles of the investigated films after treatment have been measured and no variation of the roughness has been observed after the heat treatment in H_2. The roughness of the film was measured at 30 ± 5 nm. The map of the relative heat flow measured after the heat treatment is presented in Fig. 6; as expected from Fig. 3, the number of surface defects decreases due to the heat treatment. Note that the mean relative heat flow of the film decreases slightly from 0.17 ± 0.01 to 0.15 ± 0.01 after the heat treatment. However, when compared to Fig. 3, the mean relative heat flow is higher when the film is heat-treated in H_2 than in air. The increase of the relative heat flow may be related to the formation of the Cu nanoparticles. Moreover, the absence of the roughness change after the heat treatment in H_2, as compared to the drastic roughness change (changed from 30 ± 5 to 13 ± 5 nm) when air annealed, may also be related to the formation of Cu nanoparticles as seen in Fig. 5. As seen when heat-treated in air, the film is expected to condense during the heat treatment in H_2 leading to a decrease of the film roughness. For this reason, the high value of the roughness is believed to be related to the formation of the Cu nanoparticles.

3.2. Dissolution of copper-based particles

We have established a means whereby one can manipulate the Cu_2O and Cu nanoparticles and how they were formed. In this section we discuss the results on our investigations into the dissolution of the Cu-based nanoparticles.

The films containing Cu_2O nanoparticles have been irradiated for 24 h with a continuous (cw) UV lamp with a dose = 420 J/cm^2 and for 30 min with the ns UV source with a dose = 1500 J/cm^2. No changes in coloration of the films were observed after UV irradiation. Fig. 7 presents the resulting changes of the transmission spectra of the investigated films. After cw or ns UV light exposure, the amplitude of absorption bands associated with the Cu-based nanoparticles decreases sharply. The absorption bands, which may be related to Cu_2O nanoparticles, disappeared completely when the film is irradiated overnight with the UV lamp, but still remains albeit with a lower intensity when the film is irradiated with the ns. In accordance with previous studies, the decrease of the absorption band until complete disappearance may be due to the heating of the medium that surrounds the Cu nanoparticles [21–23], to the melting of the particles [24] and also probably to the oxidation of Cu-based nanoparticles, as observed in the dissolution mechanism of Au and Ag nanoparticles [25]. Indeed, in agreement with previous study [26], the temperature of the film surface during the cw and ns light exposure is expected to increase to <300 and >2000 °C,

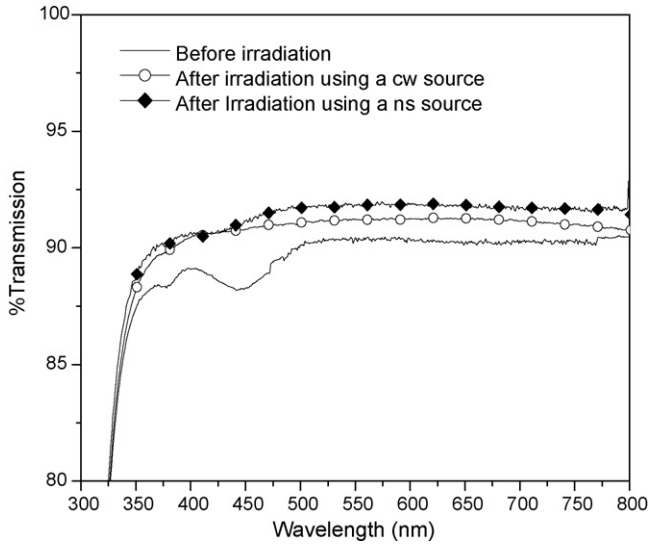

Fig. 7. Transmission spectra of films with $x = 0.05$ before and after irradiation using a cw source and ns laser irradiation.

respectively. The films have been, also, heat-treated in air for 6 h at 550 °C. Fig. 8 shows the transmission of the Cu_2O nanoparticles-containing films before and after the heat treatment. The absorption band at 440 nm probably related to the Cu_2O nanoparticles disappears after the heat treatment in air, as seen when the film is irradiated with a cw UV light confirming that the mechanism of the disappearance of the Cu-based nanoparticles is probably thermally driven. The fact that few Cu nanoparticles still remain in the film when irradiated using ns UV irradiation is probably due to the short pulse width and low repetition rate of the laser, which can allow the glass matrix heated by absorbing photon to cool down between pulses. It is also possible that as the cw lamp has no filter leading to broad band emission down to 310 nm, the strong absorption in the range ∼330 to 370 nm (FWHM) causes the heating of the film. This result is in agreement with Kapoor et al. who have shown that a pulsed Nd:YAG laser at 355 nm can cause size reduction of Cu-based nanoparticles in solution by creating a non equilibrium quasi-particle population in Cu nanoparticles [24]. The same heat treatment in air has been performed on the Cu nanoparticles-containing films. The transmission spectra of the films are presented in Fig. 9. One can notice that the amplitude of the absorption band at 580 nm which has been

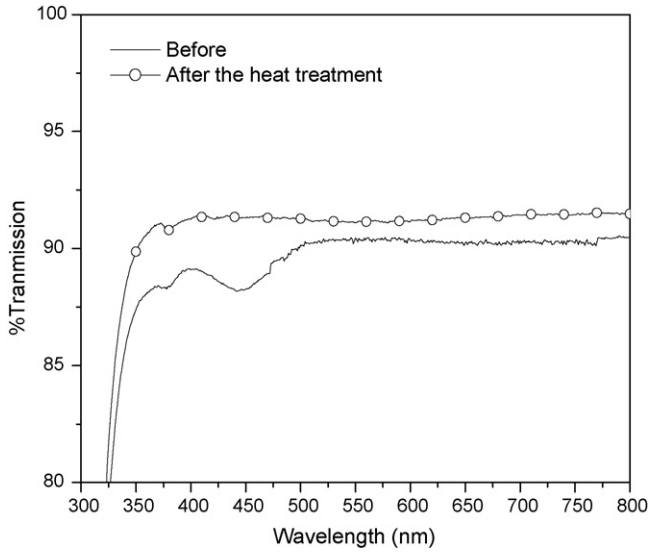

Fig. 8. Transmission spectra of films before and after the heat treatment in air for 6 h at 550 °C.

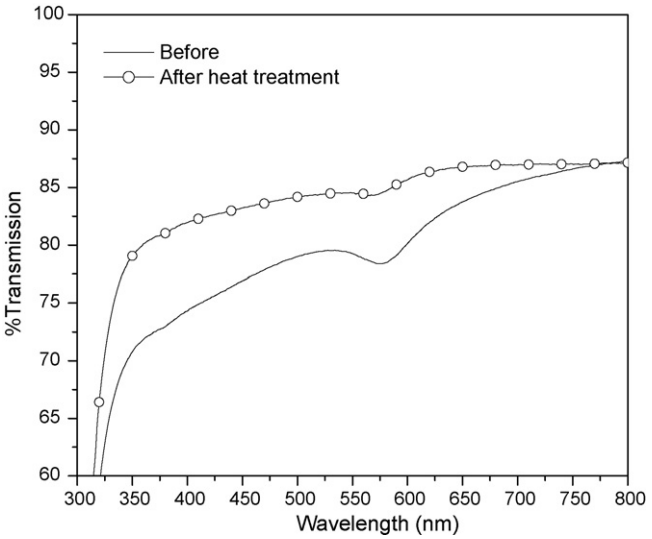

Fig. 9. Transmission spectra of heat-treated in H_2 atmosphere films with $x = 0.05$ before and after a second heat treatment in air.

related to Cu nanoparticles decreases, but still remains, indicating that the Cu nanoparticles dissolution is also driven by a thermal mechanism. However, the Cu nanoparticles dissolve much slower than the Cu_2O nanoparticles; much longer heat treatments are required to completely dissolve the pure Cu nanoparticles. This may confirm the oxidation of Cu-based nanoparticles during heat treatment in different steps. The dissolution mechanism of the Cu-based nanoparticles is still not completely understood and needs further TEM and XRD investigations.

It is also interesting to point out that no significant variation of the film mean relative heat flow has been observed after the heat treatment. This may be related to the presence of remnant Cu nanoparticles in the film. The absence of mean relative heat flow variation, when the number of Cu nanoparticles decreases, may indicate that the mean relative heat flow is sensitive to a low number of Cu nanoparticles. For future experiments, the measurement of the mean relative heat flow may be used to check the presence in low content of Cu nanoparticles, which cannot be detected using the UV–vis-NIR spectrometer. A complete study of the mean relative heat flow value as a function of the absorbance related to Cu nanoparticles is ongoing.

4. Conclusion

In this paper we have shown that we are able to form Cu_2O and Cu nanoparticles in sol–gel films deposited on microscope slides. The nature of nanoparticles formed depends on the history of the sol–gel solution used. Solutions aged for 30 min in ambient light spontaneously form Cu_2O nanoparticles, while solution aged for 1 day in darkness does not form nanoparticles, unless heated in reducing environments. Subsequent exposure of the nanoparticles impregnated films result in re-dissolution of the nanoparticles from localized heating. However, the Cu nanoparticles dissolved at much slower rates than the Cu_2O nanoparticles. Finally, we have shown that the presence in a low concentration of Cu nanoparticles in the SiO_2 film increases the relative heat flow characteristics of the films.

This study has shown that the thermal/relative heat flow characteristics can be used to detect low concentration (below optical detection limits) of Cu nanoparticles. Also we have demonstrated the feasibility of controlling the space selective formation/dissolution of the Cu nanoparticles in a single glass matrix using a UV light source with micron resolution. We expect that this laser-assisted direct metallization will play a significant role in the fabrication of integrated optical circuits and impact the optoelectronic device manufacturing and equipment industries.

References

[1] Y.S. Obeng, US Patent 6,406,609 (2002).
[2] Y.S. Obeng, IEEE Trans. Semicond. Manuf. 18 (2005) 688–694.

[3] H. Hofmeister, S. Thiel, M. Dubiel, E. Shurig, Appl. Phys. Lett. 70 (1997) 1694.
[4] F. Gonella, G. Mattei, P. Mazzoldi, C. Sada, G. Battaglin, E. Cattaruzza, Appl. Phys. Lett. 75 (1999) 55.
[5] M. Dublel, G. Mosel, J. Appl. Phys. Part 1 33 (1994) 5892.
[6] Y. Maeda, Phys. Rev. B 51 (1995) 1658.
[7] M. Ferrari, L.M. Gratton, A. Maddalena, M. Montagna, C. Tosello, J. Non-crystall. Solids 191 (1995) 101.
[8] Y. Hamana, N. Hayahsi, A. Nakamura, S. Omi, J. Lumin. 87 (2000) 859.
[9] V.N. Kalevaru, A. Benhmid, J. Radnik, B. Lucke, A. Martim, J. Catal. 243 (2006) 25–35.
[10] B. Heinrichs, F. Noville, J.-P. Pirrard, J. Catal. 170 (1997) 366.
[11] V.S. Gurin, A.A. Alexeenko, S.A. Zolotovskaya, K.V. Yumashev, Mater. Sci. Eng. C 26 (2006) 952–956.
[12] E. Cattaruzza, G. Battaglin, P. Canton, T. Finotto, C. Sada, Mater. Sci. Eng. C 26 (2006) 1092–1096.
[13] S. Lambert, C. Cellier, P. Grange, J.-P. Pirrard, B. Heinrichs, J. Catal. 221 (2004) 335–346.
[14] M. Fukushima, H. Yanagi, S. Hayashi, H.B. Sun, S. Kawata, Phys. E 21 (2004) 456–459.
[15] R. Swanepoel, J. Phys. E: Sci. Instrum. 16 (1983) 1214.
[16] E. Celik, Z. Gokcen, N.F. Ak Azem, M. Tanoglu, O.F. Emrullahoglu, Mater. Sci. Eng. B 132 (2006) 258–265.
[17] M. Cable, Z.D. Xiang, Phys. Chem. Glasses 33 (1992) 154.
[18] O.A. Yeshchenko, I.M. Dmitruk, A.M. Dmytruk, A.A. Alexeenko, Mater. Sci. Eng. B 137 (2007) 247–254.
[19] G. Battaglin, E. Cattaruzza, F. Gonella, R. Polloni, B.F. Scremin, G. Mattei, P. Mazzoldi, C. Sada, Appl. Surf. Sci. 226 (2004) 52–56.
[20] T. Lutz, C. Estournes, J.C. Merle, J.L. Guille, J. Alloy Compd. 262/264 (1997) 438–442.
[21] A. Heinglein, J. Phys. Chem. 97 (1993) 5457–5471.
[22] S. Kapoor, Langmuir 14 (1998) 1021–1025.
[23] C. Fisher, A. Henglein, J. Phys. Chem. 93 (1989) 5578–5581.
[24] S. Kapoor, D.K. Palit, Mater. Res. Bull. 35 (2000) 2071–2079.
[25] M. Mennig, M. Schmidt, H. Schmidt, J. Sol–Gel Technol. 8 (1997) 1035.
[26] L.P. Cramer, B.E. Schubert, P.S. Petite, S.C. Langford, J.T. Dickinson, J. Appl. Phys. 97 (2005) 074307.